第 31卷 第 7期
2010年 7月

Vol.31 No.7
July 2010

低合金高强度钢焊缝金属中针状铁素体的微观组织

魏 然， 吴开明
（武汉科技大学 湖北省“冶金工业过程系统科学”重点实验室，武汉 430081）

摘 要：利用光学显微镜，扫描电子显微镜及 EBSD（electron backscattering diffraction）分析技术对 800 MPa级低碳微合金高强度钢的焊缝金属进行了分析．结果表明，焊缝金属组织主要为针状铁素体和贝氏体．针状铁素体以夹杂物为核心形核，该夹杂物主要是以 Al_2O_3 为核心形成的钛氧化物．针状铁素体以夹杂物为核心多维形核呈放射状生长，仅某些方向的针状铁素体晶核迅速长大，生长方向存在取向择优．EBSD分析同样表明针状铁素体晶粒存在取向择优．观察到由同一夹杂物生长，沿同一直线方向背向生长的针状铁素体取向相同，沿不同方向生长的针状铁素体取向不同，说明其沿原奥氏体惯习面生长，并非与夹杂物共格．

关键词：低合金高强度钢；焊缝金属；针状铁素体；背散射电子衍射
中图分类号：TG142.1；TG401 文献标识码：A 文章编号：0253－360X（2010）07－0047－04


魏 然

0 序 言

对于低合金高强钢，焊缝金属的固态相变较为复杂，其最终组织取决于焊缝金属的化学成分和冷却速度，主要有先共析铁素体、侧板条铁素体、针状铁素体、贝氏体和马氏体等．其中，针状铁素体（acicular ferrite，AF）组织非常细小，且铁素体板条呈放射状生长，板条间呈大角度晶界，具有较强的抗裂纹扩展能力；可以同时改善焊缝金属的强度和韧性．当出现大量针状铁素体组织时，焊缝金属具有较高的强度和良好的低温冲击韧度．经过近些年的研究，人们对针状铁素体的形核、长大机制、转变行为特征及其组织控制取得了很多研究成果[1,2]．但是关于针状铁素体晶体学取向关系的研究仍不够充分，尚存在争议．有文献［3，4］指出，针状铁素体与原奥氏体晶粒成 Kurdjumov-Sachs（K-S）关系．同时，也有学者认为是由于与夹杂物共格或半共格促进针状铁素体形核，与晶体学取向无关[5]．晶体学取向关系不仅从根本上反映了微观组织的演变规律，而且对组织细化和性能改善有重要影响，尤其是对于大热输入焊接高强度钢的焊缝金属和热影响区的组织细化具有重要作用．文中主要通过形貌观察结合 EBSD分析对低碳微合金高强度钢焊缝金属针状铁素体组织的晶体学取向进行研究．

收稿日期：2009－02－16
基金项目：国家自然科学基金重点项目（No.50734004）

1 试验方法

试验钢板采用试验室试制的 800 MPa级低合金高强度钢，板厚 12 mm，采用气体保护焊工艺对试验钢进行焊接．试样尺寸为 150 mm×70 mm，试验时在试板上堆焊一道焊缝．焊接材料采用 WER80气体保护焊焊丝，保护气体采用 80% Ar＋20% CO_2．焊接工艺参数为：焊接电流 250 A，电弧电压 29 V，焊接速度 22 cm/min，焊接热输入为 20 kJ/cm．试验钢和焊缝金属的化学成分如表 1所示．

表 1 试验钢母材和焊缝金属的化学成分（质量分数，%）
Table 1 Chemical composition

	C	Si	Mn	P	S	Cu＋Ni＋Mo	Nb	Ti	B
母材	0.035	0.30	1.47	0.006	0.005	1.01	≤0.04	≤0.03	≤0.003
焊缝金属	0.035	0.48	1.47	0.019	0.014	1.97	0.014	≤0.05	≤0.01

试验钢板的抗拉强度为 805 MPa．经过上述工艺焊接后，焊缝金属的抗拉强度达到了 750 MPa．在焊缝金属的中心取样进行组织观察与分析．抛光好的样品用 3%的硝酸酒精溶液腐蚀后用 OLYMPUS光学显微镜观察．利用 FEI Nova400 Nano SEM扫描电子显微镜对焊缝组织进行形貌与形核的观察与分析．利用 EBSD在扫描电子显微镜下对针状铁素体的晶体学取向进行分析．

2 试验结果

2.1 光学显微组织观察

焊缝金属主要为针状铁素体和贝氏体组织，如图 1a 所示．原奥氏体柱状晶晶界上有很少量的侧板条铁素体．图 1b 中箭头 1 所指是由一个夹杂物上长出数个呈放射状铁素体板条，即魏氏体星（Widmanstätten star）．针状铁素体板条短而细，且相互交错．箭头 2 所指为另一夹杂物，两针状铁素体板条在此夹杂物上形核并背向生长．焊缝金属成分与母材接近，碳含量很低，但由于保护气氛中含有 CO_2，属于氧化性气氛，易形成大量金属氧化物促进针状铁素体形核，焊缝区原奥氏体晶粒形成非常粗大的柱状晶，晶内形核与晶界形核相比占绝对优势，促进焊缝金属形成高比例的针状铁素体．

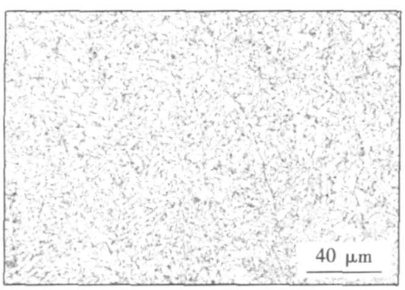

(a) 低倍

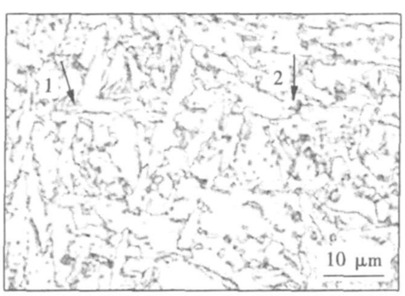

(b) 高倍

图 1 焊缝金属显微组织形貌
Fig. 1 Optical micrographs of weld metal

2.2 针状铁素体形核分析

由场发射扫描电子显微镜的观察结果（图 2）可见，针状铁素体以夹杂物为核心多维形核呈放射状生长，如图 2 箭头所指一个夹杂物上形成 3 个针状铁素体（AF1-AF3），但仅有沿某些方向生长的针状铁素体晶粒（如图 2 箭头所指 AF1，AF2）迅速长大，说明其生长方向上存在取向择优，其择优取向将在后面进一步分析．对该夹杂物进行能谱分析，得知该夹杂物含有铝，钛，锰，氧，其中铝含量较高．由于铝是比钛强的高熔点脱氧剂，通常认为氧化铝先形成，氧化钛的形成则需要过剩的氧与钛结合．因此，该夹杂物主要是以 Al_2O_3 为核心形成的钛氧化物，针状铁素体以此钛氧化物为核心形成．

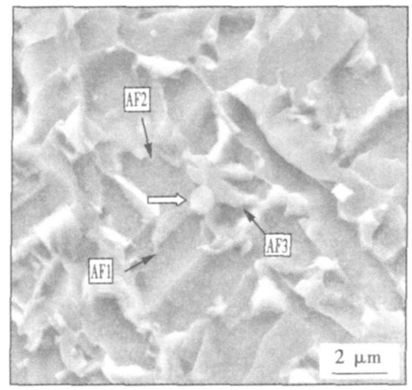

(a) 多个针状铁素体板条在一个夹杂物上形核

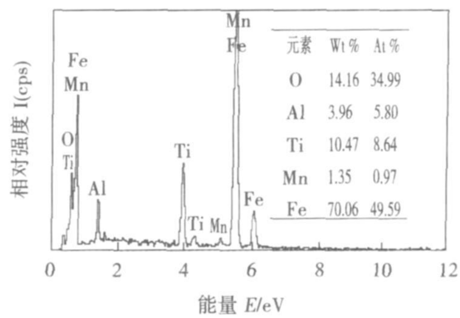

(b) 图2中白色箭头所指夹杂物的能谱分析

图 2 焊缝金属的扫描电镜观察
Fig. 2 SEM micrograph of weld metal

关于针状铁素体的形核机制，目前尚无统一的认识．其中几种主要的形核机制为：夹杂物周围奥氏体的化学成分变化促进形核；夹杂物/析出物与铁素体核心共格，从而降低形核势垒促进形核；另外，由于夹杂物与奥氏体的热收缩不一致引起的应变能，以及夹杂物作为惰性界面促进形核[6]．Ti_2O_3 上析出 MnS 而形成的贫锰区常认为是晶内铁素体形核最为有效的机理之一[7,8]，这可能是由于夹杂物中存在阳离子空位，使锰通过阳离子空位扩散进入 Ti_2O_3 夹杂物而致使 Ti_2O_3 外围生成锰贫乏区[6]，或者溶质元素在夹杂物和基体中溶解度有差异而致使 Ti_2O_3 外围生成锰贫乏区，从而促进晶内铁素体形核．关于这方面的机制，还在进行更深入的研究．

2.3 针状铁素体晶体学取向分析

图 3 为样品坐标系法向反极图．由图 3 中极密度等高线可知，晶粒取向并不随机分布，在某些晶体学方向上存在取向择优．此现象可能有两个方面的原因：（1）晶内针状铁素体与原奥氏体晶粒具有某

种取向关系，如 K-S关系；（2）晶内针状铁素体激发感生形核（Sympathetic Nucleation）[9]，即在已经形成的针状铁素体上激发形核，生成与原针状铁素体取向较为接近的二次晶内铁素体（secondary intra-granular ferrite）.

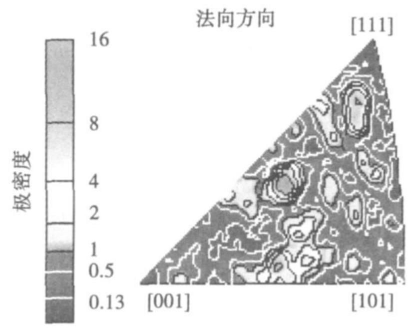

图 3　焊缝组织样品坐标系法向反极图
Fig. 3　Inverse pole map of weld metal

由取向成像图（图 4）可见，针状铁素体沿着不同的方向生长，大部分针状铁素体独立形核，各针状铁素体之间呈大角度晶界．图 4中的箭头 1所指的针状铁素体与图 1b箭头 1所指的针状铁素体形貌类似，即一个夹杂物上长出数个呈放射状铁素体板条．图 4中的箭头 2，3所指的针状铁素体与图 1b箭头 2所指的针状铁素体类似，即两针状铁素体板条在同一夹杂物上形核并背向生长．从图 4中的箭头 1，2，3所指的典型 AF均可以观察到，针状铁素体以夹杂物为核心，从同一夹杂物上长出，并且沿同一方向背向生长的针状铁素体具有相同取向，沿不同方向生长的针状铁素体具有不同取向．上述结果说明，针状铁素体沿原奥氏体某一晶向生长，与原奥氏体成某种特定的取向关系，而并非与夹杂物共格或半共格．

以上试验结果表明，焊缝区针状铁素体晶粒取向并不随机分布．可能存在铁素体与原奥氏体晶粒的某种取向关系．奥氏体的惯习面与惯习方向是 $\{111\}_\gamma$ 和 $\langle 110\rangle_\gamma$，铁素体的惯习面与惯习方向是 $\{110\}_\alpha$ 和 $\langle 111\rangle_\alpha$．一般认为，针状铁素体板条与奥氏体保持 K-S取向关系[3,4]，即：$\{111\}_\gamma /\!/ \{110\}_\alpha$；$\langle 110\rangle_\gamma /\!/ \langle 111\rangle_\alpha$．由于奥氏体 3个 $\langle 110\rangle_\gamma$ 方向上（每个方向上有 2种铁素体取向）可能有 6种不同的铁素体取向，而奥氏体的 $\{111\}_\gamma$ 晶面族中又有 4种晶面，从而铁素体共有 24种 K-S取向（变体）．吴开明与 Enomoto等[10]通过三维重建发现，铁素体板条的惯习面和惯习方向接近于 $\{111\}_\gamma$ 和 $\langle 110\rangle_\gamma$，如图 5所示[10]．

试验中，通过对焊接热影响区中由同一夹杂物

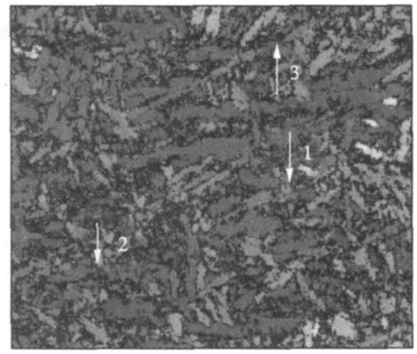

(a) 法向方向

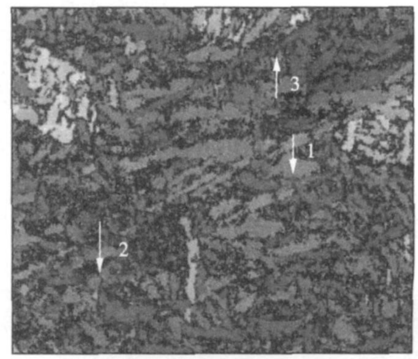

(b) 轧向方向

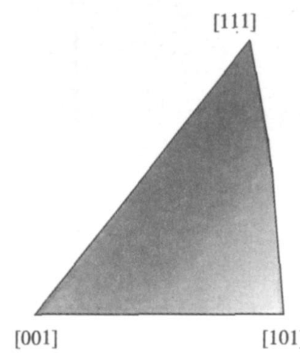

(c) 图4(a),(b)色标

图 4　焊缝金属取向成像图
Fig. 4　Orientation image map (OIM) of weld metal

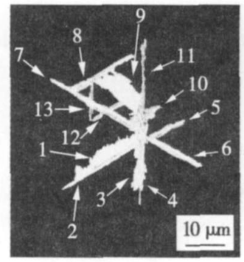

(a)

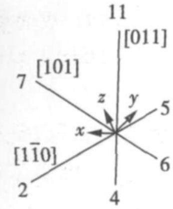

(b)

图 5　针状铁素体的三维重建表明其生长方向接近 $\langle 110\rangle_\gamma$
Fig. 5　3D-reconstructed image of acicular ferrite laths or plates, indicating that growth direction is near $\langle 110\rangle$ of austenite

上形核和生长的针状铁素体两板条间夹角的测量，发现其夹角接近 60°(图 6)，可以认为此处两针状铁素体板条沿 (111)$_\gamma$，[011]$_\gamma$ 和 [101]$_\gamma$ 方向优先生长 (夹角为 60°). 试验中很多针状铁素体板条背向生长 (图 4中箭头 2，3，图 1b中箭头 2所指)，夹角约为 180°，是 60°的整数倍，且它们具有相同的晶体学取向. 上述现象说明针状铁素体沿一定的惯习方向生长.

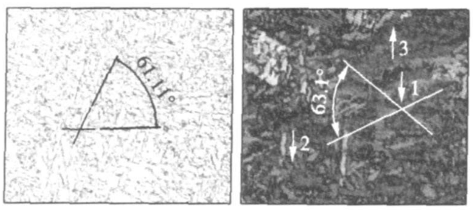

(a) 图1b中箭头1，所指针状铁素体板条间夹角　(b) 图4中箭头1，所指针状铁素体板条间夹角

图 6 针状铁素体板条间夹角示意图

Fig. 6 Angles between acicular ferrite laths or plates nucleated on inclusions in weld metal

3 结　论

(1) 以 Al_2O_3 为核心的钛氧化物周围形成的贫锰区促进焊缝中针状铁素体在同一夹杂物上多维形核，但仅有某些特定方向生长的针状铁素体得以迅速长大，生长方向上存在取向择优.

(2) 晶体学分析表明，焊缝针状铁素体晶粒取向在某些晶体学方向上存在取向择优. 晶内针状铁素体与原奥氏体晶粒很可能具有 K-S取向关系.

(3) 各针状铁素体之间呈大角度晶界，具有较强的抗裂纹扩展能力. 在同一夹杂物上长出的针状铁素体中，观察到沿同一方向背向生长的针状铁素体具有相同取向，沿不同方向生长的针状铁素体具有不同取向，说明针状铁素体沿原奥氏体的惯习面生长，而并非与夹杂物共格.

参考文献:

[1] Gutierres I, Madariaga I, Bhadeshia H K D H. Acicular ferrite morphologies in a medium carbon microalloyed steel[J]. Metallurgical and Materials Transactions A, 2001, 32(9): 2187—2196.

[2] Ricks R A, Howell P R, Barritte G S. The nature of acicular ferrite in HSLA steel weld metals[J]. Journal Materials Science, 1982, 17(3): 732—740.

[3] Watson JD, McDougall P G. The crystallography of widmanstätten ferrite[J]. Acta Metallurgica, 1973, 21(7): 961—973.

[4] Miyamoto G, Shinyoshi T, Yamaguchi J, et al. Crystallography of intragranular ferrite formed on (MnS and V(C, N)) complex precipitate in austenite[J]. Scripta Materialia, 2003, 48(4): 371—377.

[5] Ishikawa F. Intragranular ferrite nucleation in medium-carbon vanadium steels[J]. Metallurgical and Materials Transactions A, 1994, 25(5): 929—936.

[6] Bhadeshia H K D H, Honeycombe R W K. Steels microstructure and properties[M]. Third Edition. Elsevier Ltd, Oxford, UK, 2006.

[7] Gregg JM, Bhadeshia H K D H. Solid-state nucleation of acicular ferrite on minerals added to molten steel[J]. Acta Materialia, 1997, 45(2): 739—748.

[8] Shim J H, Oh Y J, Suh J Y. Ferrite nucleation potency of non-metallic inclusions in medium carbon steels[J]. Acta Materialia, 2001, 49(10): 2115—2122.

[9] Aaronson H I, Spanos G, Masamura R A, et al. Sympathetic nucleation: an overview[J]. Materials Science and Engineering B, 1995, 32(3): 107—123.

[10] Wu K M, Inagawa Y, Enomoto M. Three-dimensional morphology of ferrite formed in association with inclusions in low-carbon steel[J]. Materials Characterization, 2004, 52(2): 121—127.

作者简介：魏　然，女，1982年出生，博士研究生，讲师. 主要从事金属材料相变与组织控制研究. 发表论文 7篇.

Email: weiran@wust.edu.cn; weiranwust@sohu.com

frequency respond of sound track. Based on the above analysis, the linear generation model of arc sound was set up. The linear prediction coefficients (LPC) $\{a_i\}$, reflection coefficients and logarithm area ratio coefficients were extracted by Levinson-Durbin algorithm. In addition, the combined characteristic vector of arc sound signal was constructed.

Key words: linear prediction analysis; MIG welding; arc sound; feature extraction

Analysis on calculation accuracy and efficiency of multi-pass butt weld of pipe

YU Xingzhe[1], ZHAO Haiyan[1], LIU Li[1], LIN Jean[2] (1. Department of Mechanical Engineering, Tsinghua University & Key Laboratory for Advanced Manufacturing by Materials Processing Technology, Ministry of Education, Beijing 100084, China; 2. Beijing University of Technology, Beijing 100124, China). p39—42

Abstract: The influence of segments heat source and mesh size on calculation accuracy and efficiency of 3-D EFA of multi-pass butt welded pipe were investigated. The methods can meet the demand of calculation accuracy and high efficiency of 3D finite element simulation of large pipes. The results show that the mesh size below or equals to 3.3 mm can meet the accuracy requirement, the segment heat source, which has little efficiencies on calculation accuracy, can improve the calculations efficiency greatly.

Key words: SUS304; multi-pass butt welding; segment heat source; mesh size

Simulation of solidification microstructure evolution in molten pool of nickel base alloy

MA Rui[1], DONG Zhibo[1], WEI Yanhong[1,2], ZHAN Xiaohong[1] (1. State Key Laboratory of Advanced Welding Production Technology, Harbin Institute of Technology, Harbin 150001, China; 2. School of Material Science and Technology, Nanjing University of Aeronautics & Astronautics, Nanjing 210016, China). p43—46

Abstract: A coupled model of cellular automaton and finite difference was established and applied to solidification process in molten pool of nickel base alloy. The growth of various solidification microstructures, including planar crystal, cellular crystal, columnar dendritic crystal and crystal equiaxed dendritic in molten pool was firstly carried out and contrasted with experiment results. Moreover, variation in solidification mode in molten pool was performed, which represented cellular-to-dendritic and columnar-to-equiaxed transitions. The effect of diffusion on the distribution of solute was also calculated by solute diffusion model. The simulation results were in good accordance with the experiment results.

Key words: microstructure evolution; cellular automaton; solute segregation

Microstructural analysis of weld metal microstructures in a low carbon high strength microalloyed steel

WEI Ran, WU Kaiming (Hubei Provincial Key laboratory for System Science on Metallurgical Processing, Wuhan University of Science and Technology, Wuhan 430081, China). p47—50

Abstract: Microstructural observations and analysis of weld metal in a 800 MPa grade low carbon high strength microalloyed steel are studied by means of potical microscopy, SEM-EDS (Scanning Electron Microscopy-Electron Dispersed Spectrum) and EBBSD (Electron Backscattering Diffraction). The weld metal consists of bainite and acicular ferrite. Acicular ferrite laths or plates are nucleated on inclusions which consisted of an Al_2O_3 core and an outer layer of titanium oxide. Although multi-variant ferrite plates emanate radially from an inclusion, there are only some of them could enlengthen rapidly. It indicates growth direction of acicular ferrite preferred orientation. Results of EBSD analysis also indicate that the acicular ferrite grains in weld metal are not crystallographically oriented randomly, probably a certain orientation relationship being kept. Those acicular ferrite laths or plates nucleated on inclusions grown in opposite direction have the same orientation relationship, presumably because they have a Kurdjumov-Sachs (K-S) orientation relationship with the prior austenite grains.

Key words: high strength low alloy steel; weld metal; acicular ferrite; electron backscattered diffraction

Method of multi-classification by improved binary tree based on SVM for welding defects recongnition

LUO Aimin[1], SHEN Caihong[2], YI Bing[1], LI Kun[3] (1. School of Light Industry and Food, Sichuan University, Chengdu 610065, China; 2. Luzhou Lao Jiao Co., Ltd., Luzhou 646000, Sichuan, China; 3. School of Electronics and Information Engineering, Sichuan University, Chengdu 610064, China). p51—54

Abstract: To further recognition accuracy, the multi-classification by improved binary tree based on SVM is raised for welding defects recognition. In the welding defects classification, each class separation is computed, the classes of the two smallest class separation are trained to generate the sub-classification SVM_1 and then are combined into a new cluster G. The new cluster G and the remaining classes are computed similarly, and the second sub-classification SVM_2 and new merged cluster H are produced. This work would be repeated until the (k-1)-th sub-classification SVM is obtained and finally a balanced binary tree is come into being. Then, the optimized binary tree based on SVM by clustering is applied in welding defects recognition. The experiments show high recognition accuracy and strong generalization ability by our new algorithm.

Key words: support vector machine; class separation; binary tree; welding defects recognition

A novel high-power inverter-based resistance spot welding power supply

ZENG Min, MA Cheng, CAO Biao, FAN Fengxin (School of Mechanical and Automotive Engineering, South China University of Technology, Guangzhou 510640, China). p55—58

Abstract: To meet the welding requirements of the new materials with low resistance, a digital powerful medium frequency inverter-based resistance spot welding power is designed, with